Dissipation and variable viscosity on steady MHD free convective flow over a stretching sheet in presence of thermal radiation and chemical reaction

S. Mohammed Ibrahim

Dept. of Mathematics, Priyadarshini College of Engineering & Technology, Nellore, A.P, India
_____

ABSTRACT

A numerical analysis has been carried out on the effects of thermal radiation and viscous dissipation on steady magneto hydrodynamic free convective flow over a stretching sheet with variable viscosity in presence of chemical reaction. The governing partial differential equations are transformed to the ordinary differential equations using similarity variables, and then solved numerically by means of the fourth-order Runge-Kutta method with shooting technique. A comparison with exact solution is performed and the results are found to be in excellent. Numerical results for the velocity, temperature and concentration as well as for the skin-friction, Nusselt number, and the Sherwood number are obtained and reported graphically for various parametric conditions to show interesting aspects of the solution.
_____

INTRODUCTION

The flows due to stretching sheet in presence of electromagnetic fields are relevant to many practical applications in the metallurgy industries, polymer processing industries, paper production, filaments drawn through a quiescent electrically conducting fluid subject to a magnetic field and purification of molten metal's from nonmetallic inclusions.

Hydromagnetic flows of heat and mass transfer have become more important in recent years because of many important applications. For example, in many metallurgical processes which involve cooling of continuous strips or filaments, these elements are drawn through a quiescent fluid. During this process, these strips are sometimes stretched. The properties of the final product depend to a great extent on the rate of cooling. This rate of cooling has been proven to be controlled and, therefore, the quality of the final product by drawing such strips in an electrically conducting fluid subject to a magnetic field [1]. Liu [2] analyzed the hydromagnetic fluid flow past a stretching sheet in the presence of uniform transverse magnetic field. Chen [3] investigated the fluid flow and heat transfer on a stretching vertical sheet, and his work has been extended by Ishak et al. [4] to hydromagnetic flow. Abo-Eldahab [5] studied the hydromagnetic three dimensional flow over a stretching sheet with heat and mass transfer effects. Seddeek and Salem [6] introduced the effect of an axial magnetic field on the flow and heat transfer. Also, Seddeek and Salem [7] have analyzed the effects of variable viscosity with magnetic field on the flow and heat transfer.

Thermal radiation in fluid dynamics has become a significant branch of the engineering sciences and is an essential aspect of various scenarios in mechanical, aerospace, chemical, environmental, solar power and hazards engineering. For some industrial applications such as glass production and furnace design and in space technology applications such as cosmical flight aerodynamics rocket, propulsion systems, plasma physics and spacecraft re-entry aerothermodynamics which operate at higher temperatures, radiation effects can be significant. The effect of

246

_____

radiation on MHD flow and heat transfer problem has become more important industrially. At high operating temperatures, radiation effect can be quite significant. Many processes in engineering areas occur at high temperatures and knowledge of radiation heat transfer becomes very important for design of reliable equipment, nuclear plants, gas turbines and various propulsion devices or aircraft, missiles, satellites and space vehicles. Makinde and Ogulu [8] studied the effect of thermal radiation on the heat and mass transfer flow of a variable viscosity fluid past a vertical porous plate permeated by a transverse magnetic field. Anjali Devi and David Maxim Gururaj [9] proposed the effects of variable viscosity and nonlinear radiation on MHD flow with heat transfer over a stretching surface presence of a power-law velocity. Vidyasagar et al. [10] founded that the effects of thermal radiation and mass transfer on MHD flow over a non-isothermal stretching sheet embedded in a porous medium. Phool Singh et al [11] studied that effect of radiation and magnetic field on stretching permeable sheet in presence of free stream velocity.

In all the studies mentioned above the heat due to viscous dissipation is neglected. Gebharat [12] has shown the importance of viscous dissipative heat in free convection flow in the case of isothermal and constant heat flux at the plate. Israel-Cookey et al [13] investigated the influence of viscous dissipation and radiation on unsteady MHD free convection flow past an infinite heated vertical plate in a porous medium with time dependent suction. Suneetha et al [14] investigated radiation and mass transfer effects on MHD free convection flow past an impulsively started isothermal vertical plate with viscous dissipation. Ganeswara Reddy and Bhaskar Reddy [15] presented soret and dufour effects on steady MHD free convection flow past a semi-infinite moving vertical plate in a porous medium with viscous dissipation. Mohammed Ibrahim and Bhaskar Reddy [16] studied the radiation and mass transfer effects on MHD free convection flow along a stretching surface with viscous dissipation and heat source. Mohammed Ibrahim [17] investigated impact of heat and mass transfer effects on hydrodynamic flow past an exponentially stretching surface under the influence of viscous dissipation, heat source and thermal radiation. Vajravelu and Hadjinicolaou [18] analyzed the effects of viscous dissipation and heat source on a steady viscous fluid over a stretching sheet. Javad Alinejad and Samarbakhsh [19] initiated effects of viscous dissipation on non linear stretching sheet.

Coupled heat and mass transfer problems in presence of chemical reaction are of importance in many processes and thus have received considerable amount of attention in recent times. In processes such as drying, distribution of temperature and moisture over agricultural fields and groves of a water body, energy transfer in a wet cooling tower and flow in a desert cooler, heat and mass transfer occur simultaneously. Many practical diffusive operations involve the molecular diffusion of a species in the presence of chemical reaction within or at the boundary. Therefore, the study of heat and mass transfer with chemical reaction is of great practical importance to engineering and scientists. Afify [20] presented MHD free convective flow over a stretching surface with homogenously chemically reacting species being consumed in the process. Seddeek and Almushigeh [21] investigated the effects of radiation and variable viscosity on MHD free convection over a stretching sheet under the influence of variable chemical reaction. Alharbi et al [22] founded the Heat and mass transfer in MHD visco-elastic fluid flow through a porous medium over a stretching sheet with chemical reaction. Singh et al. [23] proposed the mass transfer effects on steady MHD convective flow along a vertical sheet in presence of chemical reaction.

However the interaction of chemical reaction and radiation effects of an electrically conducting and free convective flow past a stretching surface has received little attention. Hence, the aim of the present work is to study the effects of thermal radiation, chemical reaction, magnetic field, variable viscosity, heat source and dissipation on hydromagnetic heat and mass transfer. The governing equations are transformed by using similarity transformation and the resultant dimensionless equations are solved numerically using the Runge-Kutta fourth order method with shooting technique. The effects of various governing parameters on the velocity, temperature, concentration, skin-friction coefficient, Nusselt number and Sherwood number are shown in figures and tables and analyzed in detail.

Mathematical Formulation

Consider the steady two-dimensional laminar free convective flow heat and mass transfer over a stretching sheet. The fluid is assumed to be viscous, incompressible and electrically conducting, we also assume that the fluid properties are isotropic and constant, except for the fluid viscosity which is assumed to be an exponential function of temperature. *u, v, T* and *C* are the fluid *x* – component of velocity, *y*- component of velocity, temperature and concentration respectively.

Under the above assumptions, the two dimensional boundary layer equations for flow are given below, Ahmed [24]:

247

_____

$$\frac{\partial u}{\partial x} + \frac{\partial u}{\partial y} = 0, \tag{1}$$

$$u\frac{\partial u}{\partial x} + v\frac{\partial u}{\partial y} = \frac{1}{\rho}\frac{\partial}{\partial y}\left(\mu\frac{\partial u}{\partial y}\right) + g\beta T + g\beta^* C - \frac{\sigma B_0^2}{\rho}u, \tag{2}$$

$$u\frac{\partial T}{\partial x} + v\frac{\partial T}{\partial y} = \frac{k}{\rho c_p}\frac{\partial^2 T}{\partial y^2} - \frac{1}{\rho c_p}\frac{\partial q_r}{\partial y} + \frac{\mu}{\rho c_p}\left(\frac{\partial u}{\partial y}\right)^2, \tag{3}$$

$$u\frac{\partial C}{\partial x} + v\frac{\partial C}{\partial y} = D\frac{\partial^2 T}{\partial y^2} - Kr^*C^n. \tag{4}$$

Here, ρ is the fluid density, μ the viscosity coefficient, σ the electrical conductivity, B_0 the magnetic field of constant strength, c_p the specific heat at constant pressure, β the coefficient of thermal expansion and β^* the coefficient of concentration expansion. g is the gravitational acceleration, k is the thermal conductivity, q_r is the radiative heat flux in the y-direction, D is the mass diffusivity, n is order of reaction and Kr^* is the chemical reaction parameter. We consider the magnetic Reynolds number is very small for most fluid used in industrial applications, we assume that the induced magnetic field is negligible.

The radiating gas is said to be a non-gray if the absorption coefficient K_λ is depending on the wave length λ Abd El-Naby [25]. The equation which describes the conservation of radiative transfer in a unit volume, for all wave length is

$$\nabla.q_r = \int_0^\infty K_\lambda(T)\left(4e_{\lambda h}(T) - G_\lambda\right)d\lambda,$$

where q_r is the radiation heat flux, $e_{\lambda h}$ is the Plank's function and the incident radiation G_λ is defined as

$$G_\lambda = \frac{1}{\pi}\int_{\Omega = 4\pi} e_{\lambda h}(\Omega)d\Omega,$$

where $\nabla.q_r$ is the radiative flux divergence and Ω is the solid angle. Now, for an optically thin fluid exchanging radiation with a vertical cylinder at the average temperature value T_w and according to the above definition for the radiative flux divergence and Kirchhoff's law the incident radiation is given by

$$G_\lambda = 4e_{\lambda h}(T_w),$$

then

$$\nabla.q_r = 4\int_0^\infty K_\lambda(T)\left(e_{\lambda h}(T) - e_{\lambda h}(T_w)\right)d\lambda,$$

Expanding $K_\lambda(T)$ and $e_{\lambda h}(T_w)$ in Taylor series around T_w for small $(T - T_w)$, then we can rewrite the radiative flux divergence as

_____

$$\nabla.q_r = 4(T - T_w)\int\limits_0^\infty K_{\lambda h}\left(\frac{\partial e_{\lambda h}}{\partial T}\right)_w d\lambda,$$

where

$$K_{\lambda h} = K_\lambda(T_w).$$

Hence, an optical thin limit for a non –gray gas equilibrium, the following relation holds

$$\nabla.q_r = -4(T - T_w)\Gamma, \tag{5}$$

And, hence,

$$\frac{\partial q_r}{\partial r} = 4(T - T_w)\Gamma, \tag{6}$$

where

$$\Gamma = \int\limits_0^\infty K_{\lambda w}\left(\frac{\partial e_{\lambda h}}{\partial T}\right)_w d\lambda.$$

The boundary conditions are given by

$$u = ax, v = 0, T = T_w, \quad C = C_w \text{ as } y = 0$$

$$u = 0, \quad T = 0, \quad C = 0 \text{ as } \quad y \to \infty \tag{7}$$

where a, T_w and C_w are constants.

The continuity equation (1) is satisfied by the stream function $\psi(x, y)$ defined by

$$u = \frac{\partial \psi}{\partial y}, \quad v = -\frac{\partial \psi}{\partial x}. \tag{8}$$

To transform equations (2), (3) and (4) into a set of ordinary differential equations, the following dimensionless variables are introduced:

$$\psi = \sqrt{\frac{a\mu_0}{\rho}}xf(\eta), \eta = \sqrt{\frac{a\mu_0}{\rho}}y, \quad \theta = \frac{T}{T_w}, \quad \phi = \frac{C}{C_w}, \tag{9}$$

The variations of viscosity are written in the form Elbashbeshy et al [26]:

$$\frac{\mu}{\mu_0} = e^{-\beta\theta}, \tag{10}$$

where μ_0 is the viscosity at temperature T_w and β is the viscosity parameter.

Using these new variables, the momentum, energy and concentration equations and their associated boundary conditions can then be written as

_____

$$f''' + e^{\beta\theta}\left(ff'' - (f')^2 + Gr\theta + Gc\phi - M^2 f\right) - \beta\theta' f'' = 0, \tag{11}$$

$$\theta'' + \Pr\left(f\theta' - R(\theta - 1) + Ec f''^2\right) = 0, \tag{12}$$

$$\phi'' + Sc\left(f\phi' - Kr\,\phi^n\right) = 0. \tag{13}$$

$$f(0) = 0, \;\; f'(0) = 1 \;\; \theta(0) = 1, \;\; \phi(0) = 1,$$
$$f'(\infty) = 0, \;\; \theta(\infty) = 0, \;\; \phi(\infty) = 0, \tag{14}$$

where the prime indicates differentiation with respect to η.

$Gr = \dfrac{g\beta T_w}{a^2 x}$ (local Grashof number), $\quad Gc = \dfrac{g\beta^* C_w}{a^2 x}$ (local modified Grashof number), $\quad M = \sqrt{\dfrac{\sigma}{\rho a}}B_0$

(magnetic parameter), $\Pr = \dfrac{c_p \mu_0}{k}$ (Prandtl number), $Ec = \dfrac{a^2}{c_p T}$ (Viscous dissipation), $Sc = \dfrac{\mu_0}{\rho C_w}$ (Schmidt

number), $Kr = \dfrac{Kr^*}{aC^{1-n}}$ (non-dimensional chemical reaction parameter), $R = \dfrac{4}{a\rho c_p}$ (radiation parameter).

Fortunately, the boundary value problem (11) together with the boundary conditions (14) at $Gr = Gc = M = \beta = 0$ has an exact solution in the form:

$$f(\eta) = 1 - e^{-\eta}. \tag{15}$$

The physical quantities of interest in this problem are the skin-friction parameter C_f, local Nusselt number *Nu,* and the local Sherwood number which are defined by

$$C_f = \frac{\tau_w}{\mu\sqrt{\dfrac{a\mu_0}{\rho}}ax} = e^{-\beta\theta(\eta)}f''(0), \tag{16}$$

$$Nu = \frac{q_w}{k\sqrt{\dfrac{a\mu_0}{\rho}}T_w} = -\theta'(0), \tag{17}$$

$$Sh = \frac{m_w}{D\sqrt{\dfrac{a\mu_0}{\rho}}C_w} = -\phi'(0), \tag{18}$$

where m_w is the rate of mass flux at the wall, defined as

$$m_w = -D\left(\frac{\partial C}{\partial y}\right)_{y=0} = -D\sqrt{\frac{a\mu_0}{\rho}}C_w\phi'(0).$$

_____

The wall shear stress τ_w is given by

$$\tau_w = \mu \left(\frac{au_0}{\rho} \right)^{\frac{3}{2}} x e^{-\beta\theta(\eta)} f''(0),$$

and the heat flux q_w at the wall is given by

$$q_w = -k \left(\frac{\partial T}{\partial y} \right)_{y=0} = -k\sqrt{\frac{a\mu_0}{\rho}} T_w \theta'(0).$$

Numerical Methods

The governing boundary layer equation (11) (12) and (13) subjected to the boundary conditions (14) are solved numerically. The shooting method for linear equations is based on replacing boundary value problem by two initial value problems, and the solution of the boundary value problem is linear combination of two initial value problems. The shooting method for non-linear second order boundary values problems is similar to the linear case, accept the solution of the non-linear problem cannot be simply expressed as a linear combination between the solution of the two initial value problems. The maximum value of $\eta \to \infty$, to each group β, *M, R, n, Kr* and *Sc* determined when the value of unknown boundary conditions at $\eta = 0$ not change successfully loop with error less than 10^{-7}. Instead, we need to use a sequence of suitable values for the derivatives such that the tolerance at the end point of rage is very small. This sequence of initial values is given by secant method and we use the order Runge-Kutta method to solve the initial value problem.

RESULTS AND DISCUSSION

The results are computed for the main physical parameters which are presented by means of graphs. The influences of the thermal Grashof number *Gr*, modified thermal Grashof number *Gc,* the magnetic field parameter *M*, the viscosity parameter β, Prandtl number *Pr,* Thermal radiation parameter *R*, Viscous dissipation *Ec*, Schmidt number Sc, chemical reaction parameter *Kr* and order of the reaction parameter *n* on the velocity, temperature and concentration profiles are displayed in Figures 1 – 10. In the present study, the following default parametric values are adopted. *Gr* = 1.0, *Gc* = 1.0, *M* = 0.1, β = 0.1, *Pr* = 0.71, *R* = 0.1, *Ec*=0.01, *Sc* = 0.6, *Kr* = 0.5, *n = 1.0.* All graphs therefore correspond to these unless specifically indicated on the appropriate graph.
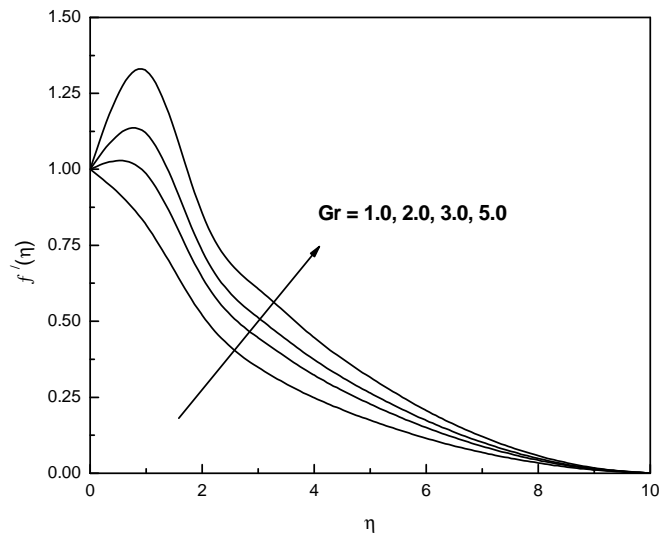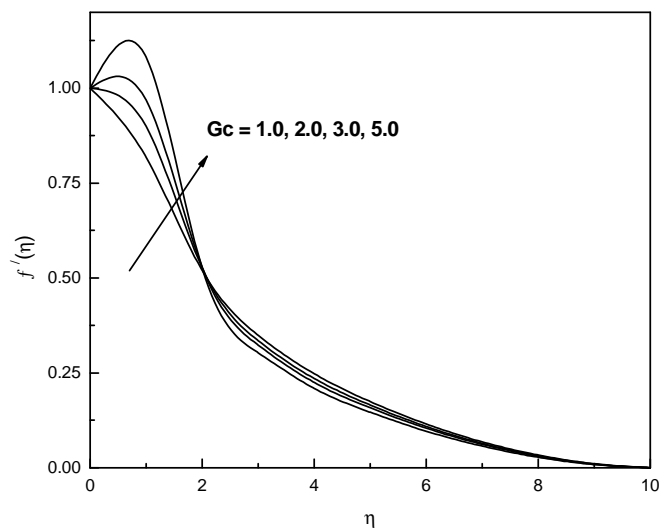
_____

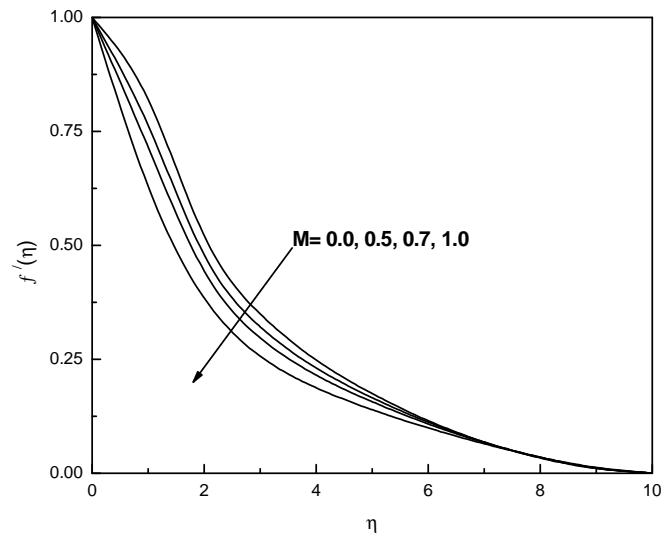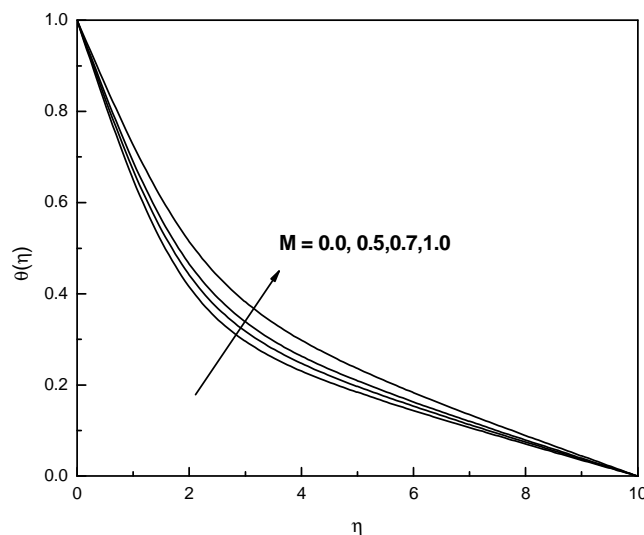**Fig. 1. Velocity profiles with different Gr**

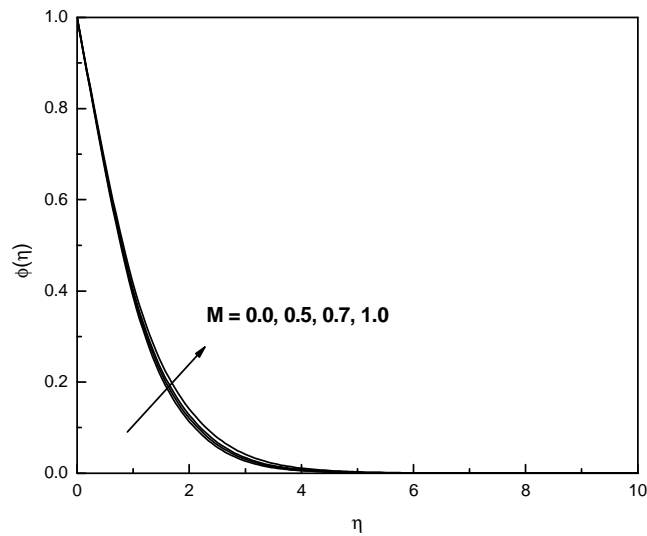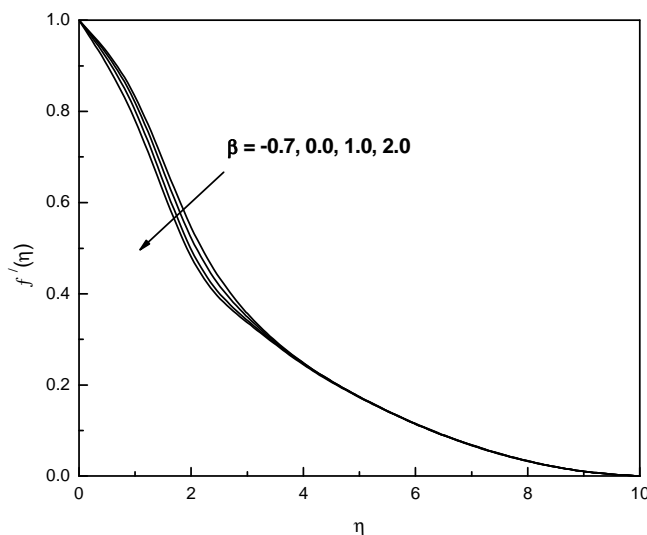**Fig.2. Velocity profiles with different Gc**

Figure 1. shows the influence of thermal buoyancy force parameter *Gr* on the velocity. As can be seen from this figure, the velocity profile increases with increases in the values of the thermal buoyancy. We actually observe that the velocity overshoot in the boundary layer region. Buoyancy force acts like a favorable pressure gradient which accelerates the fluid within the boundary layer therefore the modified buoyancy force parameter *Gc* has the same effect on the velocity as *Gr* presented in Figure 2.

Figures 3(a), 3(b) and 3(c) illustrate the influence of the magnetic parameter *M* on the velocity, temperature and concentration profiles in the boundary layer, respectively. Application of a transverse magnetic field to an electrically conducting fluid gives rise to a resistive-type force called the Lorentz force. This force has the tendency to slow down the motion of the fluid in the boundary layer and to increase its temperature and concentration. Also, the effects on the flow and thermal fields become more so as the strength of the magnetic field increases.

_____

Fig.3(a). Velocity profiles with different M

Fig.3(b)Temperature profiles with different M

The influence of viscosity parameter β on the velocity, temperature and concentration profiles is plotted in Figures. 4(a), 4(b) and 4(c) respectively. Figure 4(a) shows the velocity decreases with an increase in viscosity parameter β. It is observed that the temperature and concentration increases with an increase in viscosity parameter β.

Fig.5(a). Illustrates the velocity profiles for different values of the Prandtl number *Pr*. The numerical results show that the effect of increasing values of Prandtl number results in a decreasing velocity. From Fig.5(b), it is observed that an increase in the Prandtl number results a decrease of the thermal boundary layer thickness and in general lower average temperature within the boundary layer. The reason is that smaller values of *Pr* are equivalent to increasing the thermal conductivities, and therefore heat is able to diffuse away from the heated plate more rapidly than for higher values of *Pr*. Hence in the case of smaller Prandtl numbers as the boundary layer is thicker and the rate of heat transfer is reduced.

253

_____

Fig.3(c). Concentration profiles with different *M*

Fig.4(a). Velocity profiles with different β

The effects of the thermal radiation parameter *R* on the velocity and temperature profiles in the boundary layer are illustrated in Figures 6(a) and 6(b) respectively. Increasing the thermal radiation parameter *R* produces significant increases in the thermal condition of the fluid and its thermal boundary layer. Through the buoyancy effect, this increase in the fluid temperature induces more flow into the boundary layer thus causing the velocity of the fluid there to increase. In addition, the hydrodynamic boundary layer thickness increases as a result of increasing thermal radiation parameter *R*.

The effect of the viscous dissipation parameter i.e., the Eckert number *Ec* on the dimensionless velocity profiles and temperature are shown in Figs. 7(a) and 7(b) respectively. The positive Eckert number implies cooling of the plate i.e., loss of heat from the plate to the fluid. Hence, greater viscous dissipative heat causes a rise in the temperature as well as the velocity, which is evident from Figs. 7(a) and 7(b).
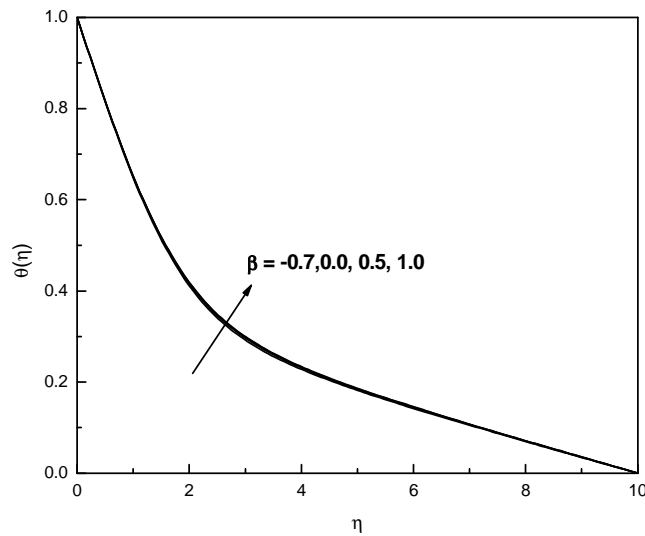
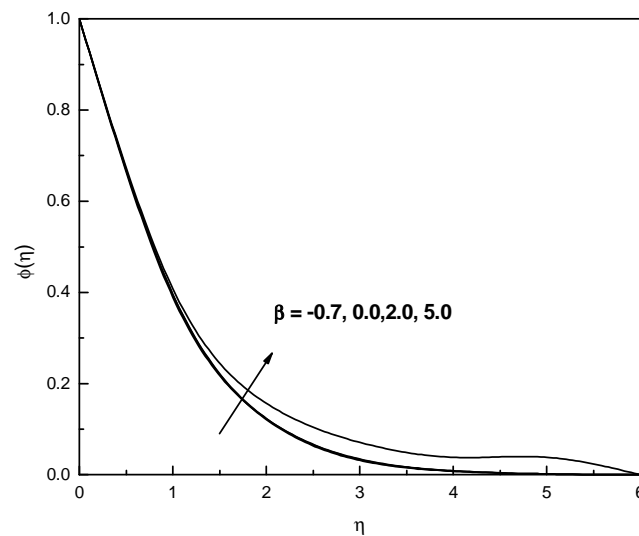_____

Fig.4(b).Temperature profiles with different β

Fig.4(c). Concentration profiles with different β

Figs. 8(a) and 8(b) display the variation of $f'(\eta)$ and $\phi(\eta)$ at different values of the Schmidt number *Sc.* It is seen that the velocity profiles and the concentration profiles are decrease as the Schmidt number *Sc* increases.

Figures 9(a) and 9 (b) display the effect of chemical reaction parameter *Kr* on velocity and concentration field. From the Figure it is observed that the velocity and concentration distribution are decreases with an increase of chemical reaction parameter *Kr*.

It is seen in Figure 10 that increases in order of reaction parameter *n* causes a marginal increase in the species concentration. Its effect on the fluid velocity and temperature is negligible and hence those figures have been not included. Therefore it is concluded that effect of parameter *n* on species consumption is not profound.
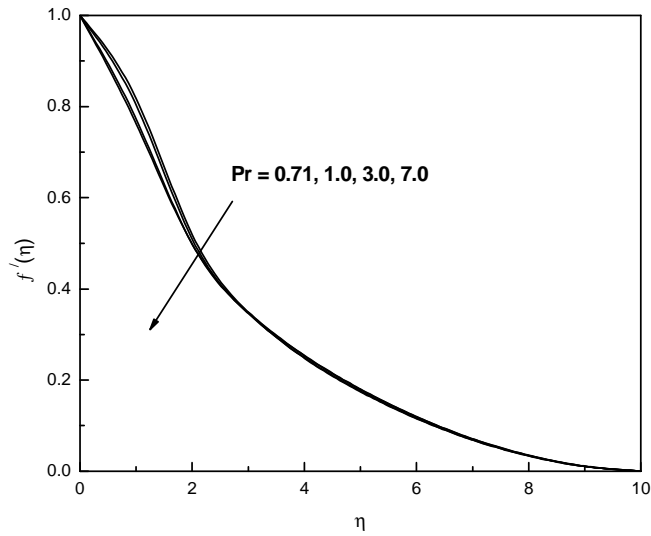
_____

Fig. 5(a). Velocity profiles with different *Pr*
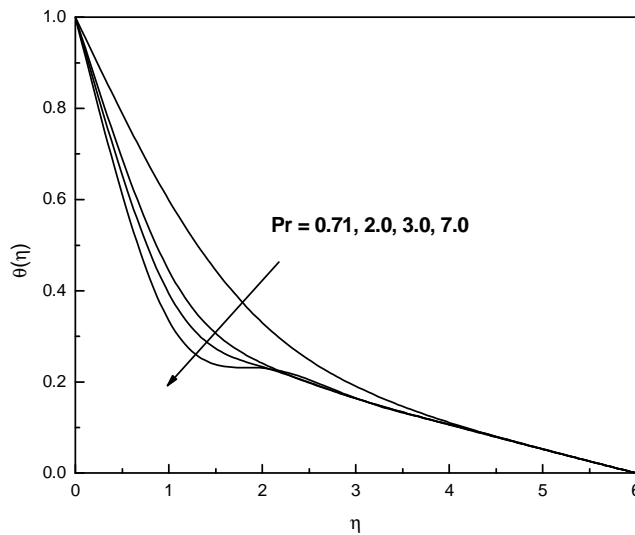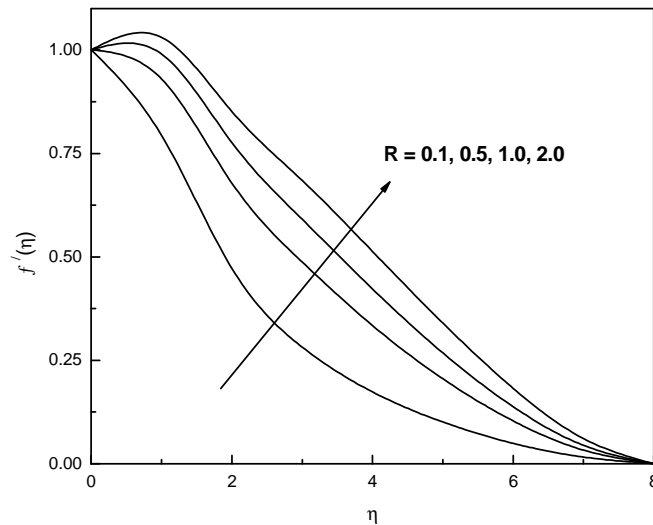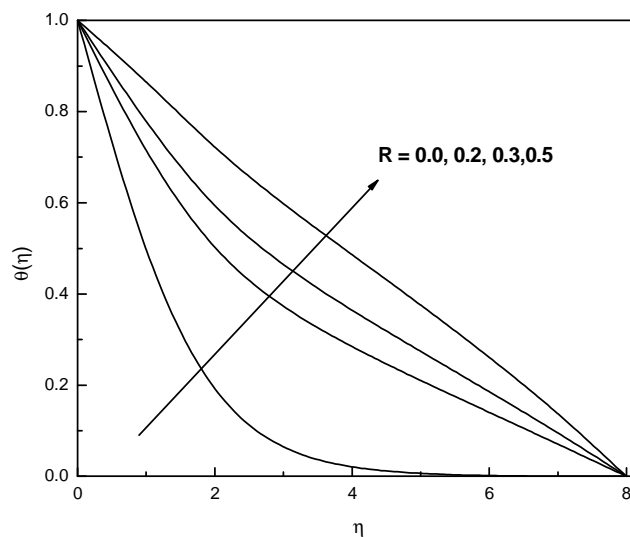

Fig.5(b). Temperature profiles with different *Pr*

Table 1: The analytical values of $f(\eta)$ in equation (15) has been presented in Table 1. The agreement between analytical and numerical solutions is excellent Values of $f(\eta)$ for different values of η at $Gr = Gc = M = \beta = 0$

η	*Exact solution in Eq.(15)*	*Present Results*
0.00	0	0
0.01	0.0099501	0.00995016
0.02	0.0198013	0.0198013
0.03	0.0295544	0.0295544
0.04	0.0392105	0.0392105
0.05	0.0487705	0.0487705

_____

Fig.6(a). Velocity profiles with different *R*

Fig.6(b). Temperature profiles with different *R*

The analytical values of $f(\eta)$ in Equation (15) has been presented in Table 1. The agreement between analytical and numerical solutions is excellent.

It is observed that with the increase in magnetic parameter that skin-friction decreases i.e. fluid experiences more and more drag as magnetic parameter increases. The heat and mass flux at surface reduce with the increase in magnetic parameter. It is noticed that with the increase in Prandtl number, skin-friction and mass flux decrease, while the heat flux increases at the Prandtl number increases. The skin friction and Sherwood number increase as the radiation parametet increase, while the Nusselt number decreases as radiation parameter increases. Also the skin-friction, Nusselt number and Sherwood number decrease when viscosity parameter increases. As Eckert number increase heat flux is decreases, while skin-friction and mass flux are increase. It is seen from Table 4 that as the Schmidt number or chemical reaction parameter increases the skin-friction decreases, while the surface temperature

_____

and mass flux at the surface increase. As the order of reaction parameter increases skin-friction and heat flux increases, while mass flux is decreases.
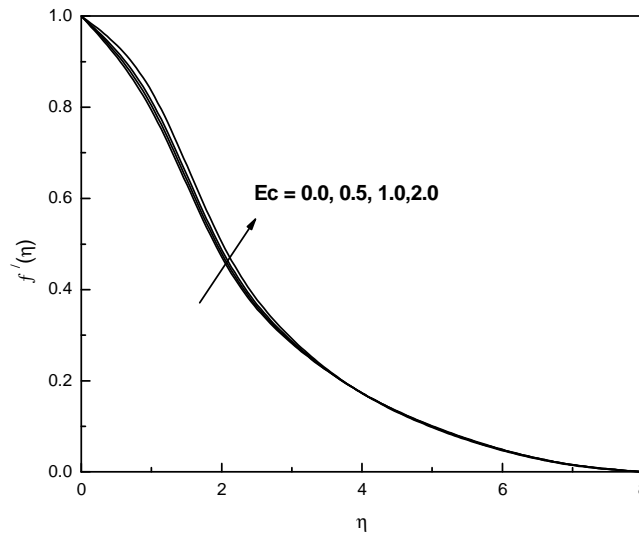

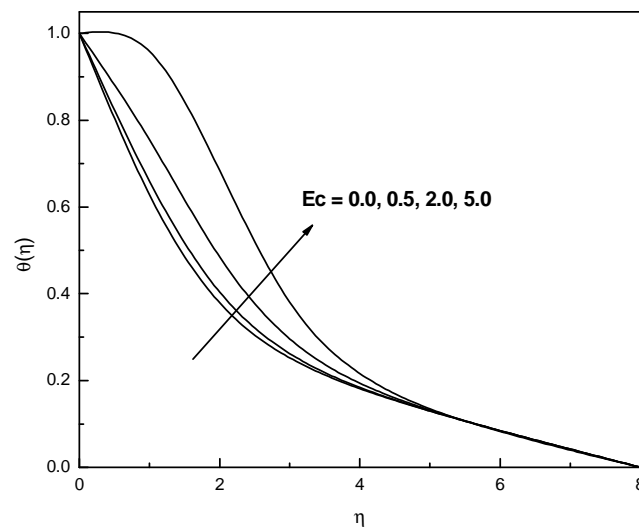**Fig.7(a). Velocity profiles with different *Ec***

Fig. 7(b). Temperature profiles with different *Ec*

Table 2. Values of $f''(0), -\theta'(0)$ and $-\phi'(0)$ for different values of *Pr = 0.71, R = 0.1, Ec = 0.01, Sc = 0.6, Kr = 0.5, n = 1.0.*

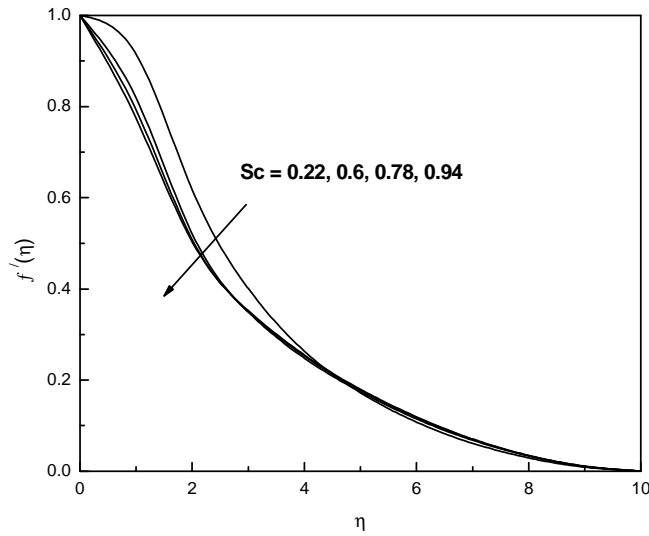| *Gr*	*Gc*	*M*	β	$f''(0)$	$-\theta'(0)$	$-\phi'(0)$
1.0	1.0	0.1	0.1	0.126129	0.379284	0.784181
2.0	1.0	0.1	0.1	0.653068	0.44163	0.812883
3.0	1.0	0.1	0.1	1.1347	0.484738	0.835481
1.0	2.0	0.1	0.1	0.555957	0.408217	0.801812
1.0	3.0	0.1	0.1	0.968104	0.432905	0.817571
1.0	1.0	0.3	0.1	0.0755175	0.372216	0.781026
1.0	1.0	0.5	0.1	-0.0221643	0.358435	0.774969
1.0	1.0	0.1	0.3	0.17723	0.378836	0.784516
1.0	1.0	0.1	0.5	0.138245	0.338583	0.781979

_____

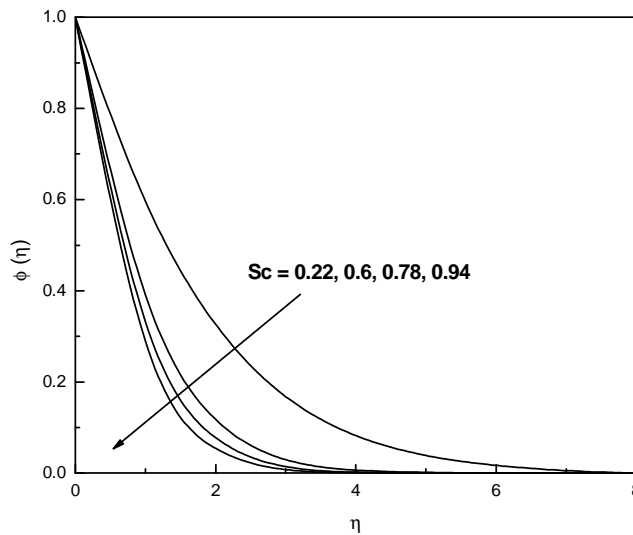**Fig.8(a). Velocity profiles with different *Sc***

Fig.8(b). Concentration profiles with different *Sc*

Table 3. Values of $f''(0), -\theta'(0)$ and $-\phi'(0)$ for different values of *Gr =1.0, Gc =1.0, M = 0.1,* β *= 0.1, Sc = 0.6, Kr = 0.5, n = 1.0.*

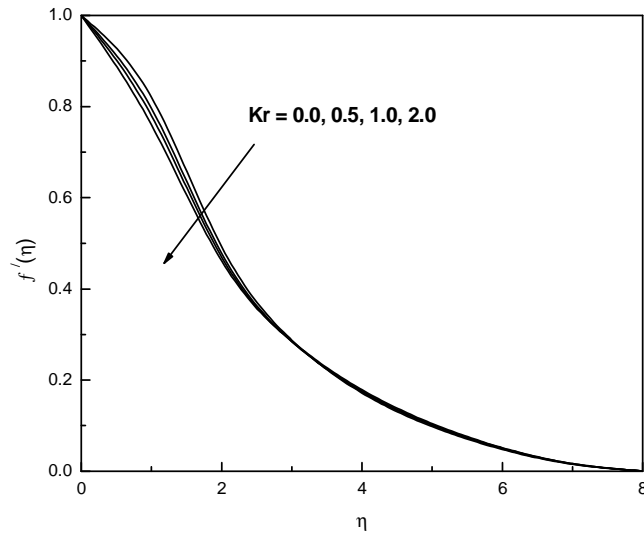| Pr	R	Ec	$f''(0)$	$-\theta'(0)$	$-\phi'(0)$
0.71	0.1	0.01	0.126129	0.379284	0.784181
1.0	0.1	0.01	0.103827	0.437067	0.781886
2.0	0.1	0.01	0.0613488	0.58023	0.778189
0.71	0.3	0.01	0.226872	0.207293	0.797753
0.71	0.5	0.01	0.28211	0.110184	0.80487
0.71	0.1	0.03	0.126723	0.377643	0.784242
0.71	0.1	0.05	0.127316	0.376002	0.784303

_____
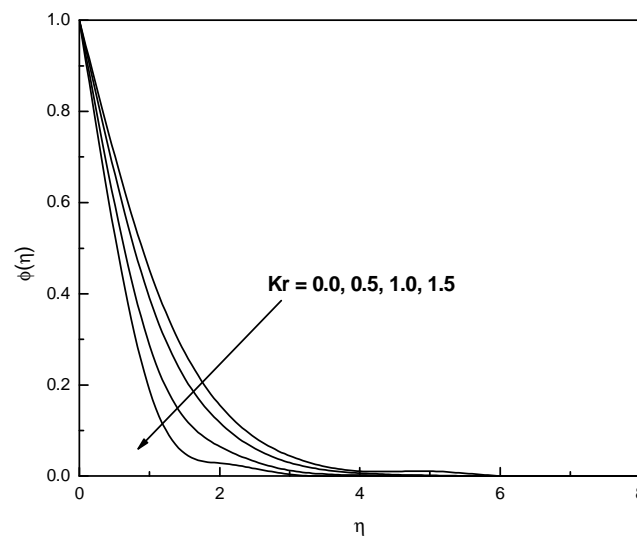

Fig.9 (a). Velocity profiles with different *Kr*

Fig. 9(b). Concentration profiles with different *Kr*

Table 4. Values of $f''(0), -\theta'(0)$ **and** $-\phi'(0)$ **for different values of** *Gr = Gc =1.0, M = β =0.1, Pr = 0.71, R = 0.1, Ec = 0.01*

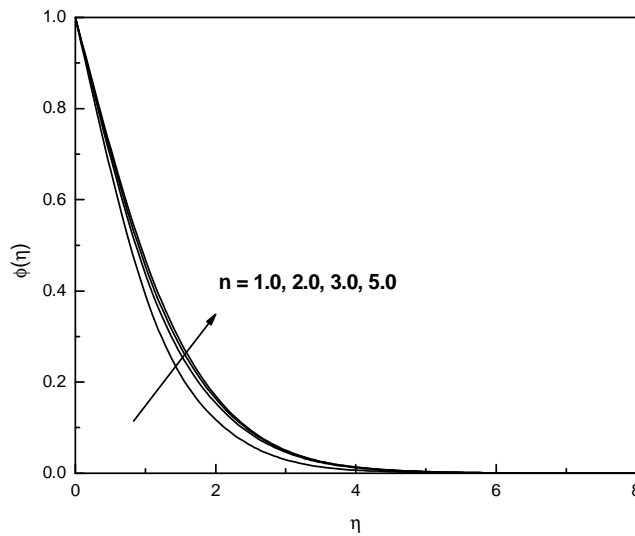| Sc	Kr	n	$f''(0)$	$-\theta'(0)$	$-\phi'(0)$
0.6	0.5	1.0	0.126129	0.379284	0.784181
0.78	0.5	1.0	0.0989485	0.373746	0.89766
0.94	0.5	1.0	0.0795652	0.370259	0.98788
0.6	1.0	1.0	0.0970533	0.368095	0.953008
0.6	2.0	1.0	0.0568926	0.374284	1.22555
0.6	0.5	2.0	0.146653	0.383946	0.714913
0.6	0.5	3.0	0.154531	0.385365	0.681773

_____

Fig. 10. Concentration profiles with different *n*

REFERENCES

[1]. Vajravelu K, Hadjinicolaou, *Int. J. Engg. Sci*. **1997**, 35,1237.

[2]. Liu, I.C. *International Communications in Heat and Mass Transfer*, **2005**, 32, 1075.

[3]. Chen, C.H., *Heat and Mass Transfer*, **1998**, 33, 471.

[4]. Ishak, A., Nazar, R., & Pop, I. *Heat Mass Transfer*, **2008**, 44, 921.

[5]. E.M. Abo-Eldahab, *Heat Mass Transfer*, **2005**, 41,734.

[6]. Seddeek, M. A., Salem, A. M. *computational Mechanics*, **2007**, 39, 401.

[7]. Seddeek, M. A, and Salem, A. M. *Physics Letters A*, **2006**, 353, 337.

[8]. Makinde, O.D and A. Ogulu , *Chemical Engineering Communications*, **2008**, 195(12) , 1575.

[9]. Anjali Devi S.P and David Maxim Gururaj, *Advances in Applied Science Research*, **2012**, 3(1), 319.

[10]. Vidyasagar G., Bala Anki Reddy P., Ramana B and Sugunamma V, *Advances in Applied Science Research*, **2012**, 3(6), 4016.

[11]. Phool Singh., Ashok Jagid., Tomer N.S and Deepa Sinha, *Int.J. of. Inf & Math. Sci*., **2010**, 6(3), 160.

[12]. Gebharat B , *J..Fluid Mech.,* **1962**, 14, 225.

[13]. Israel-Cookey C Ogulu A and Omubo-Pepple VB, *Int.J.Heat Mass Transfer*, **2003**, 46, 2305.

[14]. Suneetha S Bhaskar Reddy N and Ramachandra Prasad V, *Thermal Science* , **2009**, 13(2), 171.

[15]. Ganeswara Reddy M and Bhaskar Reddy N, *Int. J. of Appl. Math and Mech*. **2010**, 6(1), 1.

[16]. Mohammed Ibrahim S and Bhaskar Reddy N , *Int. J. of Appl. Math and Mech*. **2011**, 8(8), 1.

[17]. Mohammed Ibrahim S, *Journal of Global Research in Mathematical Archives,* **2013**, 1(8), 67.

[18]. Vajravelu K and Hadjinicolaou A , *Int. Comm. Heat and Mass,* **1993***, 20(3),* 417.

[19]. Javad Alinejad and Samarbakhsh S , *Journal of Applied Mathematics,* **2012**, Article ID 587834, 10.

[20]. A.A. Afify, *Heat Mass Transfer*, **2004**, 40, 495.

[21]. Seddeek M.A and Almushigeh A.A ,*Appl.Appl.Math*. **2010**, 5(1), pp. 181.

[22]. Alharbi S., Bazid M.A.A and El Gendy M S , *Applied Mathematics*, **2010**, 1, 446.

[23] Singh G., Sharma P.R and Chamkha A.J, *International Journal and Technology*, **2012**, 4(20), 1.

[24]. Ahmed A., *Heat and Mass Transfer*, **2004**, 40, 495.

[25]. Abd El-Naby, M. A., Elbarbary Elsayed, M. E., Abdelazem Nader, Y., *Applied Mathematics and Computation*, **2004**, **151,** 327–346.

[26]. Elbashbeshy, E. M. A. and Ibrahim, F. N. , *J. Phys. D: Appl. Phys*., 26, 2137.